

Research report

# Preparation of thermally induced SCC samples

Risto Ilola, Ahmed Mazhar, Iikka Virkkunen

## Table of contents

1 Introduction .....	3
2 Experimental .....	3
2.1 Test material and sample manufacturing .....	3
2.2 Residual stress .....	3
2.3 Metallography and hardness testing .....	4
3 Results .....	5
3.1 Residual stresses .....	5
3.2 Hardness .....	6
3.3 Microstructure .....	8
3.4 SCC tests .....	8
4 Conclusions .....	8
5 References .....	8

## 1 Introduction

This technical report presents the research done within the TOFFEE project WP3, Thermally induced stress corrosion cracking, during 2023 at Aalto University. The research in TOFFEE WP3 focuses on investigation of the role of thermal loads in promoting SCC.

## 2 Experimental

### 2.1 Test material and sample manufacturing

Two rings of 150 mm in length of austenitic 316L stainless steel pipe (diameter 326 mm, thickness 33 mm) were received from VTT. The material represents the material used in OL3 primary cooling circuit. Chemical composition of the pipe material is presented in Table 1.

The 150 mm long pipe rings were welded together at Suisto Engineering with NG-GTAW method using 316LSi filler metal (Table 1). The welding was done according to a WPS received from TVO, so that the weld represents the OL3 primary circuits welds.

Table 1. Chemical composition of the pipe material and filler metal. /1/

	C	Mn	Si	P	S	Cr	Ni	Mo	Cu	N
Base material	0.028	1.81	0.39	0.022	0.002	17.1	12.03	2.27	0.56	0.08
Filler metal	0.02	1.8	0.85	0.023	0.002	18.3	11.4	2.5	0.2	0.073

Two segments of 140 mm x 65 mm in size were sawed from the welded pipe for SCC tests, segment 1 to VTT and segment 2 to Aalto. Prior to the SCC tests, thermal loading was introduced to the weld segments using induction heating. In the thermal loading, the peak temperature of 500°C was reached in 4 s during heating, and it was followed by air cooling for 30 s. The cycle was repeated for 3 times.

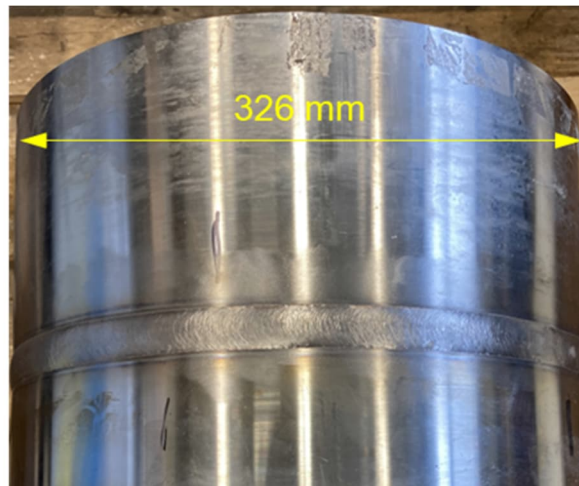


Figure 1. 316L pipe welded with NG-GTAW method.

### 2.2 Residual stress

The residual stresses after thermal cycling were measured from the weld segments using Stresstech XStress 3000 G2R diffractometer with a MnK $\alpha$  X-ray tube. Measurements were done from the inner side of the pipe (weld root side) at the weld fusion line, and at 5 and 25 mm distances from the weld fusion line in phi 0° (axial), phi 45°, and phi 90° (hoop) directions (Figure 2).

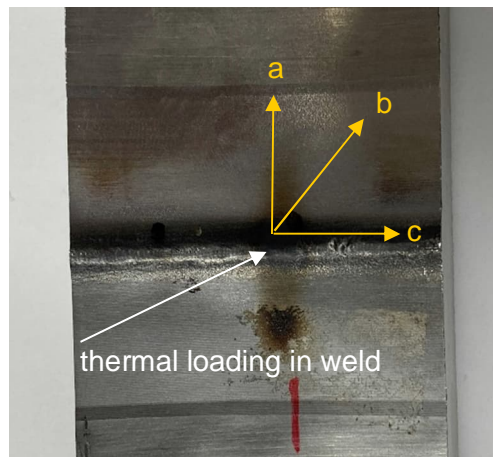


Figure 2. Location of the thermal cycling, residual stress measurement, and the direction of the residual stress measurements: a)  $\phi 0^\circ$  (axial), b)  $\phi 45^\circ$ , and c)  $\phi 90^\circ$  (hoop) direction.

### 2.3 Metallography and hardness testing

A metallographic sample of the weld cross-section was prepared for measurement of the weld hardness profile and metallographic investigation. The sample was ground and polished mechanically, and the etched with a Beraha II etchant. Hardness profile was measured from the root and bead sides of the weld, and from the middle of the weld (Figure 3) using Duramin-40 AC2 hardness tester with a HV1 scale (1 kg load). The distance between measurement point was 1 mm.

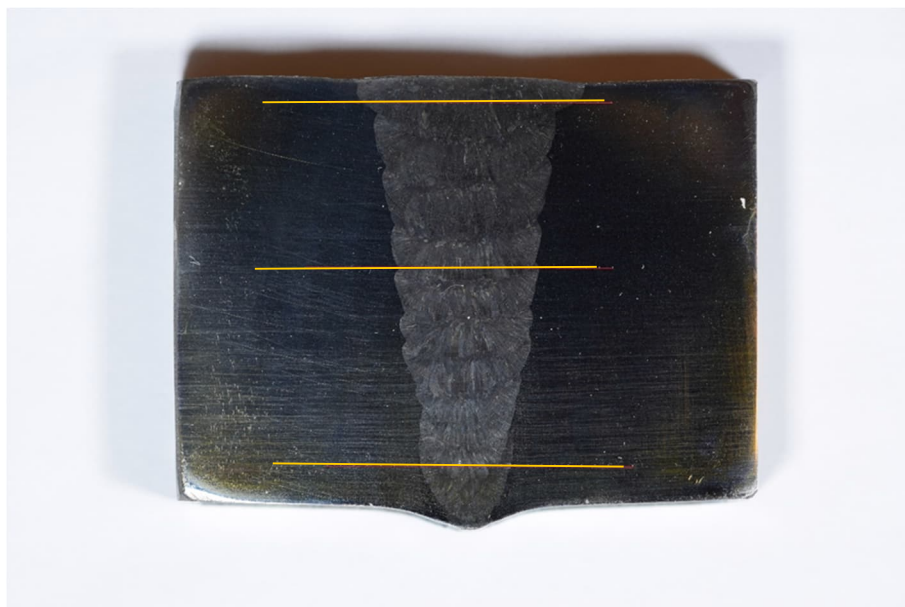


Figure 3. Location of hardness measurement lines in the pipe weld cross-section.

### 3 Results

#### 3.1 Residual stresses

The measured residual stresses in the welded pipe segments 1 and 2 after thermal cycling are presented in Table 2. Thermal cycling produced maximum axial tensile residual stresses of order of 500 MPa at the distances of 0 and 5 mm from the weld fusion line. Tensile residual stresses at the same distances from the weld fusion line in a non-thermally cycled location were considerably lower. The hoop residual stresses were generally lower at the thermally cycled locations, but in the non-thermally cycled locations there was anomaly in the results. There was variation in the residual stress values in both segments, but it can be considered typical to residual stress measurements.

Table 2. Results of the residual stress measurements.

Phi (degree)	Segment	Distance from weld fusion line (mm)	Thermal loading peak temperature (C)	Residual stress (MPa)	Variation +/- (MPa)
0	1	0	500	562	56
45				416	42
90				268	20
0	1	5	500	673	14
45				514	20
90				341	25
0	1	25	500	-182	9
45				23	16
90				206	14
0	1	0	No	-15	50
45				149	34
90				63	17
0	1	5	No	-20	8
45				172	18
90				293	13
0	1	25	No	-121	14
45				69	69
90				282	282
0	2	0	500	454	54
45				304	46
90				166	15
0	2	5	500	449	17
45				405	11
90				285	18
0	2	0	No	205	20
45				50	23
90				90	11
0	2	25	No	-739	36
45				-649	28
90				-356	46

### 3.2 Hardness

Hardness profiles measured from different locations of the weld cross-section are presented in Figure 4. Hardness values were the greatest in the weld root location being of order of 250 HV1 at maximum. The lowest hardness values were measured on the bead side of the weld. The hardness of the base material was below 200 HV1, which is typical for the pipe material in solution annealed and quenched condition.

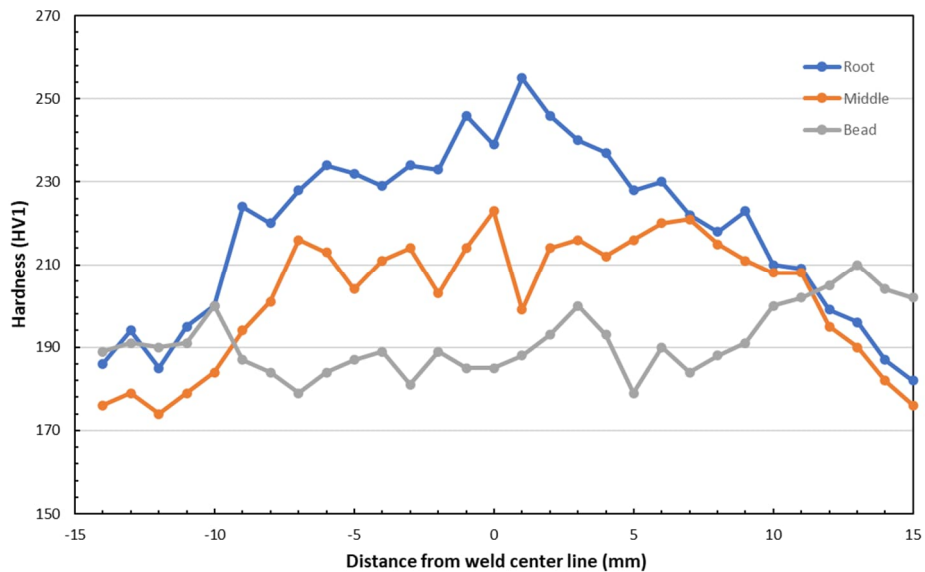


Figure 4. Hardness profile of the weld measured from the root side, bead, and middle of the weld.

Table 3. Hardness values (HV1) in the different positions of the weld cross-section and location of the measurement (BM = base material, W =weld).

Distance from weld centre line (mm)	Root	Point location	Middle	Point location	Bead	Point location
-14	186	BM	176	BM	189	BM
-13	194	BM	179	BM	191	BM
-12	185	BM	174	BM	190	BM
-11	195	BM	179	BM	191	BM
-10	200	BM	184	BM	200	BM
-9	224	BM	194	BM	187	BM
-8	220	BM	201	BM	184	BM
-7	228	BM	216	BM	179	BM
-6	234	BM	213	BM	184	W
-5	232	BM	204	BM	187	W
-4	229	BM	211	W	189	W
-3	234	BM	214	W	181	W
-2	233	W	203	W	189	W
-1	246	W	214	W	185	W
0	239	W	223	W	185	W
1	255	W	199	W	188	W
2	246	W	214	W	193	W
3	240	W	216	W	200	W
4	237	BM	212	W	193	W
5	228	BM	216	W	179	W
6	230	BM	220	W	190	W
7	222	BM	221	BM	184	W
8	218	BM	215	BM	188	BM
9	223	BM	211	BM	191	BM
10	210	BM	208	BM	200	BM
11	209	BM	208	BM	202	BM
12	199	BM	195	BM	205	BM
13	196	BM	190	BM	210	BM
14	187	BM	182	BM	204	BM
15	182	BM	176	BM	202	BM

### 3.3 Microstructure

Microstructure of the weld photographed from the middle of the pipe weld cross-section is presented in Figure 5. The microstructure was uniform throughout the weld having a typical dendritic weld microstructure.

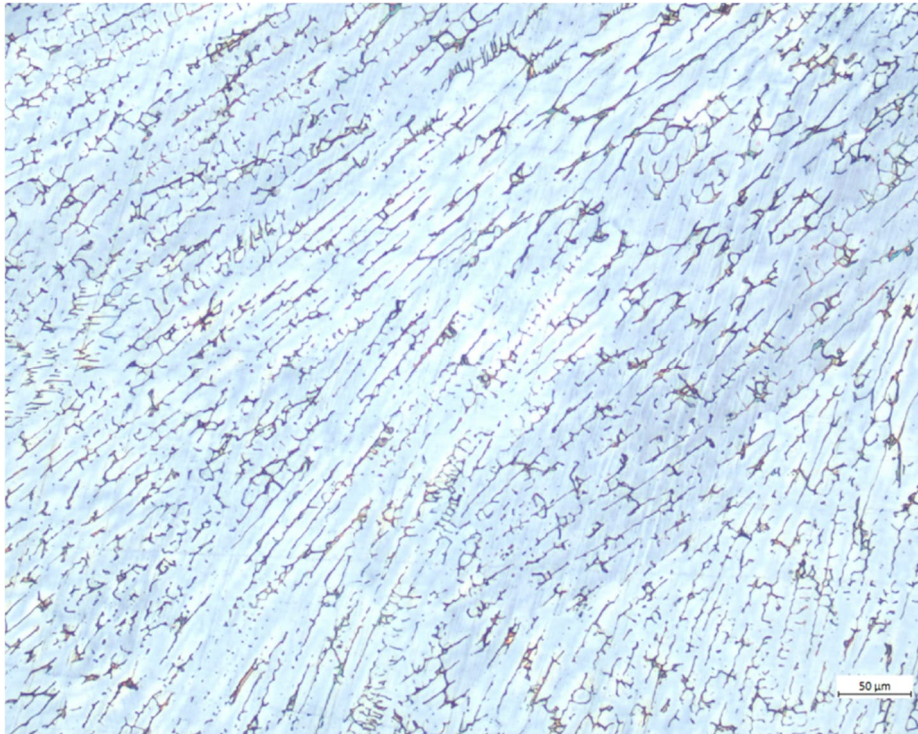


Figure 5. Microstructure in the middle of the pipe weld cross-section.

### 3.4 SCC tests

The original plan in the in the TOFFEE project WP3 was to study the SCC susceptibility using autoclave tests for thermally loaded SCC samples. For technical and other unexpected reasons, the autoclave testing has been delayed. The aim is to start these tests during spring 2024. Due to uncertainty of these tests, parallel SCC tests will be done at Aalto University. The tests are ambient temperature SCC tests in an aqueous solution of sulphuric acid and potassium tetrathionate /2/. The tests started in January 2024.

## 4 Conclusions

This research report contains the first results in TOFFEE project WP3, Thermally induced SCC samples. Research on residual stress fields in the weld is still in progress. A more comprehensive analysis of the results will be reported in a M.Sc. thesis this spring.

## 5 References

/1/. Seppänen, T., Alhainen, J., Arilahti, E., Solin, J, Vanninen, R., and Pulkkinen, E. EPR Piping Material Study: Basic Characterization and Low Cycle Fatigue at Room Temperature. Proceedings of the ASME 2022 Pressure Vessels & Piping Conference, PVP2022, July 17-22, 2022, Las Vegas, Nevada, USA, 6 p.

/2/. Breimesser, M., Ritter, S., Seifert, H.-P., Suter, T., and Virtanen, S. Application of Electrochemical Noise to Monitor Stress Corrosion Cracking of Stainless Steel in Tetrathionate Solution Under Constant Load. Corrosion Science 63 (2012), p. 129–139.